RESEARCH ARTICLE

Modelling the degradation of Sunset Yellow FCF azo dye by Fe_2O_3/ Bentonite catalyst using artificial neural networks

Mohammad Ehsan Mosayebian[2], Reza Moradi [1*], Kazem Mahanpoor [3]

[1] *Department of Chemistry, Tuyserkan Branch, Islamic Azad University, Tuyserkan, Iran*

[2] *Department of Electrical Engineering, Tuyserkan Branch, Islamic Azad University, Tuyserkan, Iran*

[3] *Department of Chemistry, Arak Branch, Islamic Azad University, Arak, Iran*

ARTICLE INFO

Article History:
Received 2021-04-27
Accepted 2021-07-12
Published 2021-08-01

Keywords:
Fe2O3/Bentonite
Artificial neural network
photocatalyst
Sunset Yellow FCF

ABSTRACT

In this paper, the precipitation method has been used to stabilize Fe_2O_3 particles on Bentonite zeolite (BEN). Fe_2O_3/BEN catalysts have been characterized by scanning electron microscopy (SEM), X-ray diffraction (XRD) and Brunauer-Emmett-Teller (BET) surface area analysis. Artificial neural network (ANN) was used for modelling the photocatalytic degradation of Sunset Yellow FCF (SYF) azo dye in aqueous solution under irradiation in the batch photoreactor. The parameters including pH, catalyst amount, dye concentration and H2O2 concentration were applied as input; the output of the network was degradation percentage. Modelling the results the photocatalytic degradation of dye using a feed forward, back propagation three-layer network, topology (4:7:1) with four neurons in the input layer, seven neurons in the hidden layer and one neuron in the output layer were used. Comparison between data obtained from ANN and experimental data indicated that the proposed ANN model provides reasonable predictive performance. The optimum conditions were as follows: pH= 4, catalyst amount=60 mg/L, dye concentration =50 ppm and H_2O_2 concentration =32 ppm. The chemical oxygen demand (COD) analysis of the dye under optimum conditions showed 91% reduction in 80 min period.

How to cite this article
Mosayebian M.E., MoradiR., Mahanpoor K. Modelling the degradation of Sunset Yellow FCF azo dye by Fe_2O_3/Bentonite catalyst using artificial neural networks . J. Nanoanalysis., 2021; 8(3): 209-220. DOI: 10.22034/jna.006.

INTRODUCTION

Colorants are either dyes or pigments. The terms are often used indiscriminately; in particular, pigments are quite often considered to be a subgroup of dyes. Pigment particles have to be attached to substrates by additional compounds, like a polymer in paint, a plastic, or a melt. These are finely divided solids, the average particle size of which can vary from 0.2 to 10 micrometers. They may be inorganic or organic. Dyes, on the other hand, are applied to various substrates (textile materials, leather, paper, etc.) from a liquid in which they are completely, or at least partially, soluble. Unlike pigments, dyes must possess a specific affinity to the substrates for which they are used [1]. Colored wastewaters are one of the most toxic compounds of industries which can cause problems in healthy human and environment [2-4]. Therefore, degradation or removal of dyes is necessary.

The advanced oxidation process (AOP) of photocatalytic mechanism type was used for degradation of dye [5]. The enhanced activity of the UV/Fe_2O_3/BEN system is due to the well-known electron excitation from the valance band to the conduction band of the semi-conducting oxide to give electron–hole pairs. Photocatalyst mechanism was used for the study since by exposing ultraviolet radiation to the semiconducting oxides; valance electrons can be transferred to conduction bands. During this transition, some holes are created in the valance band and additional electrons are also created in the conduction band. Dissolved oxygen molecules in water take extra electrons from the

* Corresponding Author Email: *reza.moradi_bi@yahoo.com*

Table 1. The chemical compounds of BEN.

Formula	Conc.%
Na_2O	3.39
MgO	1.23
Al_2O_3	11.03
SiO_2	65.35
SO_3	1.26
Cl	0.21
K_2O	1.72
CaO	0.20
TiO_2	0.20
Fe_2O_3	1.49
BaO	0.48
Loss of ignition (L.O.I)	13.40

conduction band and after certain reactions, radical hydroxide will be released. On the other hand, after reaction with several holes the water molecules and the hydroxide ions are created in the valance band, thus hydroxide radicals are created. Finally, hydroxide radicals with organic pollutants react and cause the breakdowns and failures, thus convert them into minerals [6-8].

Zeolites are crystalline solids with small holes and channels of 3 to 10 Å. They are classified into natural and synthetic categories. Sodium, potassium, magnesium, calcium or other cations and water molecules are also found in the structure of these compounds [9].

The ANN are, as their name indicates, computational networks, which attempt to simulate, in a gross manner, the networks of nerve cells (neurons) of the biological (human or animal) central nervous system. This simulation is a gross cell-by-cell (neuron-by-neuron, element-by-element) simulation. It borrows from the neurophysiological knowledge of biological neurons and of networks of such biological neurons. It thus differs from conventional (digital or analog) computing machines that serve to replace, enhance or speedup human brain computation without regard to organization of the computing elements and of their networking [10]. The ANN comes from the intended analogy with the functioning of the human brain adopting simplified models of biological neural network. The human brain consists of nearly 1011 neurons of different types. In a typical neuron, one can find nucleus with which the connections with other neurons are made through a network of fibres called dendrites. Extending out from the nucleus is the axon, which transmits, by means of a complex chemical process, electric potentials to the neurons, with which the axon is connected to. When signals, received by neuron, become equal or surpass their threshold values, it triggers sending an electric signal of constant level and duration through axon. In this way, the message is transferred from one neuron to the other. In the ANN, the neurons or the processing units may have several input paths corresponding to the dendrites. The units combine usually by a simple summation, that is, the weighted values of these paths. The weighted value is passed to the neuron, where it is modified by threshold function such as sigmoid function. The modified value is directly presented to the next neuron. An ANN consists of a pool of simple processing units, which communicate by sending signals to each other over a large number of weighted connections [11-14].

In this paper, synthesized Fe_2O_3/BEN particles by precipitation method were characterized by SEM, XRD and BET. The effects of operational parameter such as pH, catalyst amount, dye concentration and H_2O_2 concentration on the process were studied. ANN with topology (4:7:1) was used for modelling the photocatalytic degradation of SYF.

EXPERIMENTAL

Materials

The raw materials were BEN (Kani Kav Kashan Company, Iran) extracted from deposits in the region of Kashan. BEN chemical compounds are shown in Table 1.

Table 2. The structure and characteristics of SYF dye.

Dye	Structure	λmax(nm)	MW(g/mol)	C.I.
Sunset Yellow FCF (SYF)	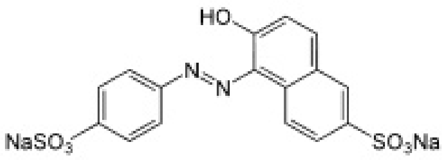	482	452.36 452.36	15985

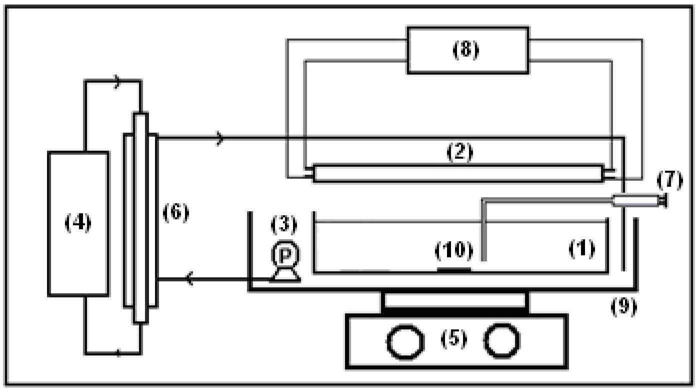

Fig. 1. Schematic diagram of batch photoreactor.

(1)Batch reactor, (2) UV Lamp, (3) Water pump, (4) thermo bath, (5) Heater and stirrer, (6) Heat exchanger, (7) Sampling system, (8) Electronic supply, (9) Water jacket, (10) Magnetic bar.

The azo dye, SYF was obtained from Aldrich Company and was used without further purification. The structure and characteristics of SYF are shown in Table 2. The pH values were adjusted at the desired level using dilute NaOH 0.1N and H_2SO_4 0.1N. Other materials such as $Fe(NO_3)_3.9H_2O$, C_2H_5OH and H_2O_2 were all Merck products (Germany). Double distilled water was used for preparation of requisite solutions.

Equipments

Fig. 1 shows the schematic diagram of batch photoreactor which was used for photocatalytic degradation of dye. In this equipment, the total volume of photoreactor was 1 L with a lamp (mercury 15W, low pressure, Philips) was used in photoreactor. UV/Vis Spectrophotometer, Jenway (6505) was employed to measure the absorbance using glass cells of path length 1 cm. For COD measurement, COD meter analyzer model AL250 AQUALYTIC was used. XRD analysis of the samples was done using a X-ray diffractometer Philips-XPert MPD, tube: Co kα, wavelength: λ=1.78897Å, Voltage: 40 kV, Current: 30 mA. The morphologies and specific surface areas of the catalyst were taken by SEM model Philips XL30 and Micrometric-100E Brunauer Emmett Teller (BET). pH values were measured with a Horiba M12 pH meter.

Synthesis of Fe_2O_3/BEN catalyst

For preparing of catalyst, 200 ml saturated solution of $Fe(NO_3)_3.9H_2O$ were prepared and 100 g BEN was added slowly and mixing for 2 h with magnetic stirring. 50 ml NaOH solution 1 M and 10 ml H_2O_2 (30%) dropwise was added, the sediment obtained by using filter paper, smooth, primarily washed three times by ethanol. The precipitated was then given a deposition for 2 h at a temperature of 100 °C inside the oven and then for 4 h at a temperature of 400 °C within the furnace. The precipitation was sieved using 100 mesh standard sieve.

Procedure

For the photodegradation of SYF, solutions containing various concentrations of dye and catalyst were prepared. The suspension pH values were adjusted at the desired levels using dilute H_2SO_4 0.1N and were allowed to equilibrate for 30 min in darkness. Then, the prepared suspension was transferred to batch reactor and H_2O_2 added to the solution. The degradation reaction took place under the radiation of a mercury lamp. The concentration of the samples was determined (at 5 min intervals and centrifuged with centrifuge 4232 ALC) using a spectrophotometer (UV-Vis spectrophotometer, Jenway (6505) at λ_{max}= 482 nm. The photodegradation (X) as a function of time is given by Equation (1):

$$X = \frac{C_\circ - C}{C_\circ}, \tag{1}$$

Where C_o and C are the concentration of dye at $t = 0$ and t, respectively.

The ANN description

An ANN is an information-processing system that has certain performance characteristics in common with biological neural networks. ANNs have been developed as generalizations of mathematical models of human cognition or neural biology, based on the assumptions that:

1. Information processing occurs at many simple elements called neurons.
2. Signals are passed between neurons over connection links.
3. Each connection link has an associated weight, which, in a typical neural net, multiplies the signal transmitted.
4. Each neuron applies an activation function (usually nonlinear) to its net input (sum of weighted input signals) to determine its output signal.

A neural network is characterized by (1) its pattern of connections between the neurons (called its architecture), (2) its method of determining the weights on the connections (called its training, or learning, algorithm), and (3) its activation function.

A neural net consists of a large number of simple processing elements called neurons, units, cells, or nodes. Each neuron is connected to other neurons by means of direct communication links, each with an associated weight. The weights represent the information being used by the net to solve a problem. Neural nets can be applied to a wide variety of problems, such as storing and recalling data or patterns, classifying patterns, performing general mappings from input patterns to output patterns, grouping similar patterns, or finding solutions to constrained optimization problems [15].

Each neuron has an internal state, called its activation or activity level, which is a function of the inputs it has received. Typically, a neuron sends its activation as a signal to several other neurons. It is important to note that a neuron can send only one signal at a time, although that signal is broadcast to several other neurons.

A layered feed-forward neural network has layers, or subgroups of processing elements. A layer of processing elements makes independent computations on data that it receives and passes the results to another layer. The next layer may in turn make its independent computations and pass on the results to yet another layer. Finally, a subgroup of one or more processing elements determines the output from the network. Each processing element makes its computation based upon a weighted sum of its inputs. The first layer is the input layer and the last the output layer. The layers that are placed between the first and the last layers are the hidden layers. The processing elements are seen as units that are similar to the neurons in a human brain, and hence, they are referred to as cells, neuromimes, or artificial neurons. A threshold function is sometimes used to qualify the output of a neuron in the output layer [16].

For all data sigmoid transfer function [17] in the hidden layer and a linear transfer function in the output node were used. All calculations were carried out with Matlab mathematical software with the ANN toolbox.

RESULTS AND DISCUSSION

The characterization of Fe_2O_3/BEN catalyst

Fig. 2 shows the SEM images of (a) BEN and (b) Fe_2O_3 particles have loaded on the surface of BEN (Fe_2O_3/BEN). It seems that the iron oxide particle take place on the surface of BEN. The BET results indicate that the surface area of BEN has decreased (from 267 m^2/g to193 m^2/g) then being stabilized Fe_2O_3 on BEN. To reveal the interaction between

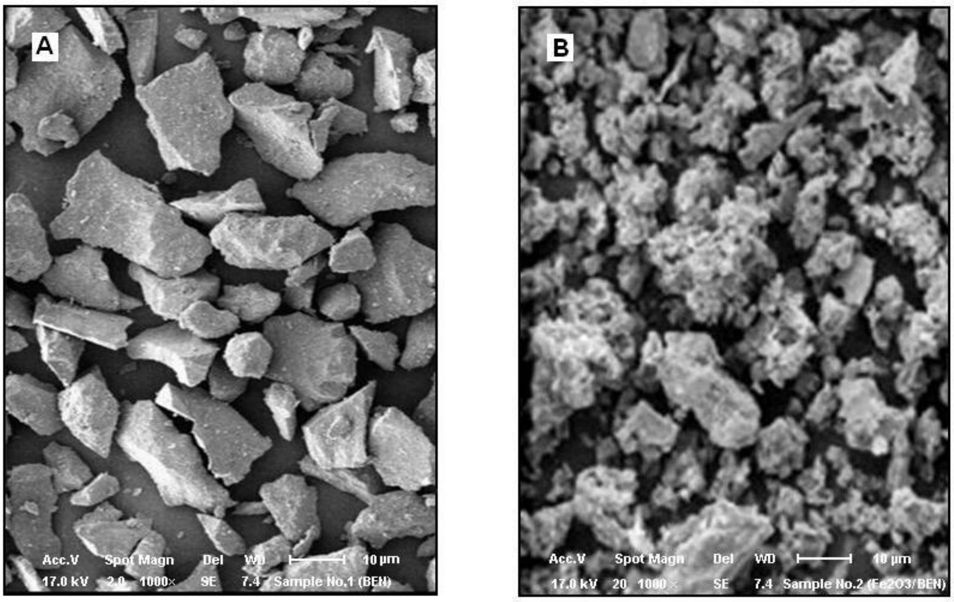

Fig. 2. SEM images of (A) BEN, (B) Fe_2O_3/BEN.

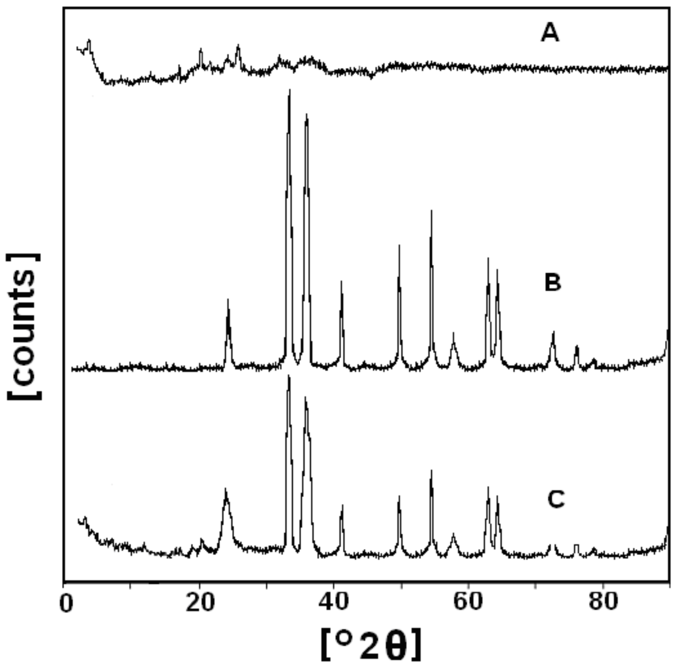

Fig. 3. XRD pattern of (A) BEN, (B) Fe_2O_3 particles and (C) Fe_2O_3/BEN.

the Fe_2O_3 and the BEN, the crystal structures of the raw BEN and the Fe_2O_3/BEN calcined at 400 ^{O}C after 4 h were measured as is shown in Fig. 3. The XRD patterns of samples are illustrated in Fig. 3. XRD patterns of the as-prepared samples (2θ ranges from 10° to 80°). Clearly the XRD patterns of Fe_2O_3/BEN consist of the raw BEN which can be calcined at 400 ^{O}C for 4 h. It is implied that the frame structure of zeolite after Fe_2O_3 loading will not be destructed and less amount of Fe_2O_3 has

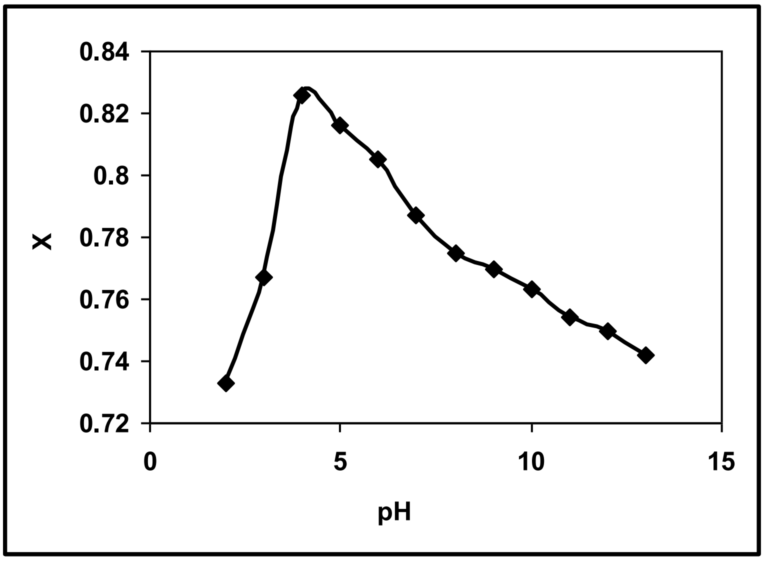

Fig. 4. Effect of pH on the degradation of dye (catalyst amount=60 mg/L, dye concentration=50 ppm, H_2O_2 concentration =32 ppm).

loaded on BEN. The comparison of XRD patterns of Fe_2O_3 [18] before and after being calcined at 400 ^{O}C indicated that the crystalline phase of the prepared Fe_2O_3 (supported on BEN) and BEN was stable during the heat treatment process. The crystallite size of Fe_2O_3/BEN was calculated using the Debye-Scherer Equation [19]:

$$D= 0.9 \lambda / \beta \cos\theta, \quad (2)$$

where D is the average crystallite size, λ is the wavelength of Co kα , β is the full width at half maximum (FWHM) of the diffraction peaks, and θ is the Bragg's angle. The average crystallite size of Fe_2O_3 supported on BEN was estimated about 115 micrometers.

The effect of pH

pH is one of the main factors influencing the rate of dye degradation in the photocatalytic process. Fig. 4 shows the photodegradation of SYF at different pH from 2 to 13, which clearly shows the best results obtained in an acidic solution (pH= 4, X= 0.826). The degradation of dye decreased with increasing of pH value from 5 to 13. The reason it is that, there is the photocatalytic degradation of SYF in acidic solutions, which is probably due to the formation of hydroxyl radical ($OH^{\bullet}$) as it can be inferred from the following reactions [20, 21]:

$$e_{CB}^{-} + O_2 \rightarrow O_2^{\bullet -} \quad (3)$$

$$O_2^{\bullet -} + H^{+} \rightarrow HO_2^{\bullet} \quad (4)$$

$$2HO_2^{\bullet} \rightarrow O_2 + H_2O_2 \quad (5)$$

$$H_2O_2 + O_2^{\bullet -} \rightarrow OH^{\bullet} + OH^{-} + O_2 \quad (6)$$

As pH increases, the hydroxyl radicals concentration decreases and therefore, dye degradation decreases.

The effect of catalyst amount

Fig. 5 shows the effect of catalyst amount on dye degradation. According to Fig. 5 from 30 to 60 mg/L catalyst amount the degradation trend shows an increase. One explanation would be to attribute the number of active sites on catalyst surface be directly proportional to the degrees of photocatalytic degradation. However, at catalyst amounts within 60 to 85 mg/L range, the trend of SYF degradation follows gradual decrease. This observation confirms the fact that the light scattering phenomenon occurred in a collision with catalyst particles in solution and loses the amount of light photons energy and thus decreases the photocatalytic reaction rate [22, 23]. Maximum degradation of SYF occurs at 60 mg/L catalyst dosage.

The effect of dye concentration

The effect of dye concentration in the range of 10 to 65 ppm on degradation efficiency is shown

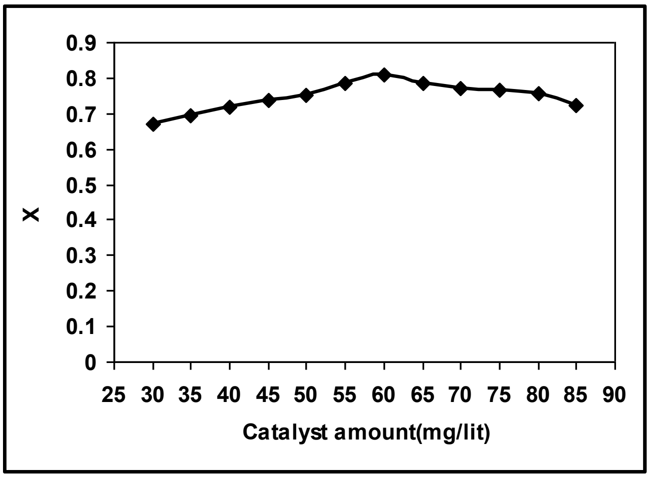

Fig. 5. Effect of catalyst amount on the degradation of dye (pH=4, dye concentration=50 ppm, H_2O_2 concentration =32 ppm).

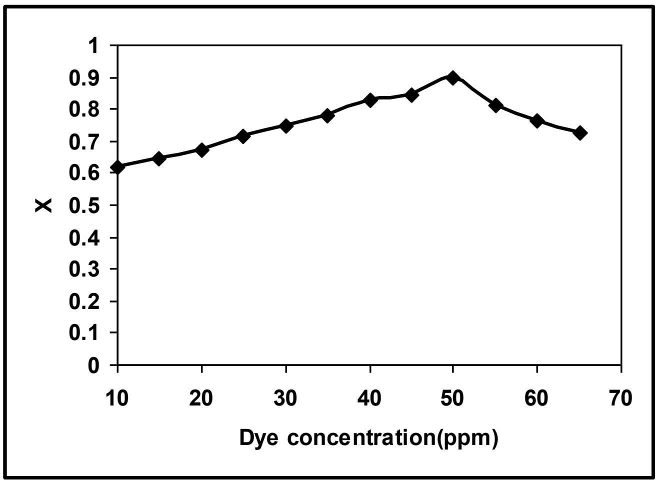

Fig. 6. Effect of dye concentration on the degradation process (pH=4, catalyst amount =60 mg/L, H_2O_2 concentration =32 ppm).

in Fig. 6. The degradation of dye approaches maximum at 50 ppm dye concentration. At lower dye concentrations than 50 ppm, degradation is directly proportional to dye concentration. This trend however, alters beyond 50 ppm dye concentrations. The presumed reason is that when the initial concentration of dye is increased, more and more dye molecules are adsorbed on the surface of the catalyst. The large amount of adsorbed dye is thought to have an inhibiting effect on the reaction of dye molecules with photogenerated sites or hydroxyl radicals, which is due the lack of any direct contact between them. Once the concentration of dye is increased, it also causes the dye molecules to adsorb light and the photons never reach the catalyst surface, thus the degradation efficiency decreases [24].

The effect of H_2O_2 concentration

Fig. 7 addresses to the variation of SYF degradation subject to changes in H_2O_2 concentration in the range of 4 to 48 ppm. The results indicate that maximum degradation of dye under irradiation i.e. 0.922 would be achieved and corresponds to 32 ppm H_2O_2 concentration. In the primary zone of 4 to 32 ppm H_2O_2 concentration, degradation of dye increases with increasing in H_2O_2 concentration. This can be explained by the effect of the additionally produced hydroxyl radicals. In the zone with higher concentrations

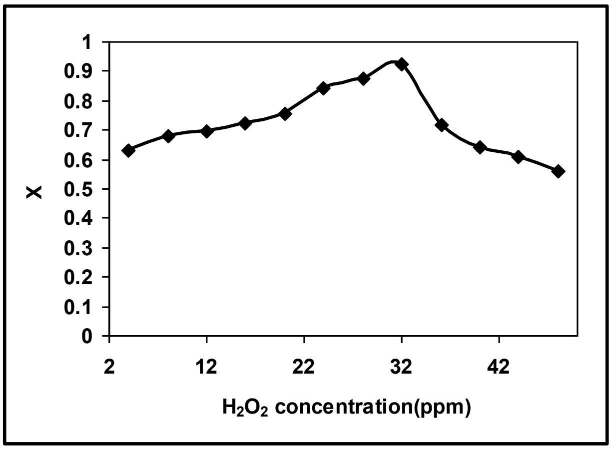

Fig. 7. Effect of H_2O_2 concentration on the degradation of dye (pH=4, catalyst amount =60 mg/L, dye concentration =50 ppm).

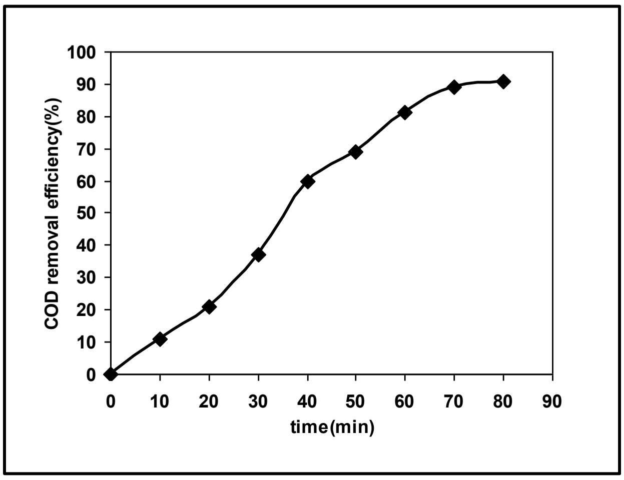

Fig. 8. COD removal efficiency of dye (pH=4, catalyst amount =60 mg/L, dye concentration=50 ppm, H_2O_2 concentration =32 ppm).

than 32 ppm reduction in degradation efficiency is observed. This indicates that the excess amount of H_2O_2 is decomposed without promoting further degradation or maybe due to recombination of hydroxyl radicals and also reaction of hydroxyl radicals with H_2O_2, the concentration of $OH^{\bullet}$ and so degradation efficiency is decreased. Therefore, the optimal amount of H_2O_2 concentration is 32 ppm [25, 26].

The photocatalytic mineralization of dye

The COD test is commonly used to indirectly measure the amount of organic compounds in color wastewaters. The COD test was used to confirm that the organic pollutants are decomposed and are converted into mineral. The results of such experiments are shown in Fig. 8. The degradation of dye under optimal operational conditions and the removal 91% from organic pollutants have been performed in 80 min period. The results can be confirmed by the decomposition of organic matter that was present in the dye sample. The COD removal efficiency (%) has been calculated by Equation (7) [27]:

$$COD \text{ removal efficiency (\%)} = \frac{COD_0 - COD}{COD_0} \times 100 \qquad (7)$$

Where COD_o and COD are COD values at $t = 0$ and t, respectively.

The ANN model

In this study, the net used to be feed-forward

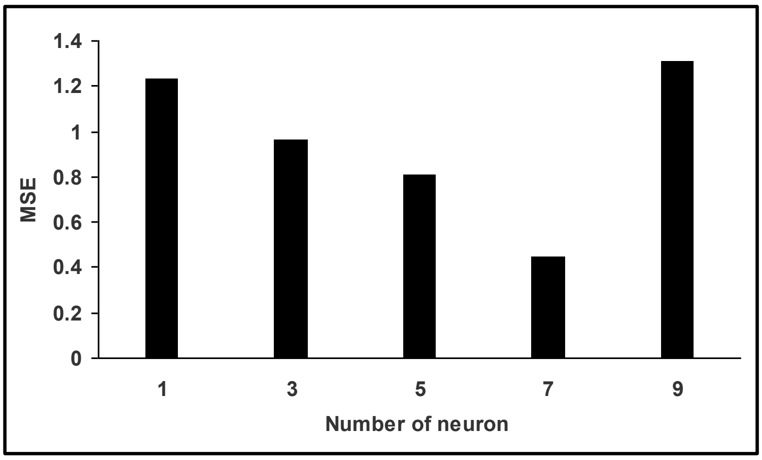

Fig. 9. The MSE value and number of neurons in the hidden layer for dye.

neural network trained by backpropagation algorithm. The input parameters to neural network were: pH, catalyst amount, dye concentration, H_2O_2 concentration and output of the network were degradation percentage.

The topology of an ANN is determined by the number of layers, the number of nodes in each layer and the nature of the transfer functions. Optimization of ANN topology is probably the most important step in the development of a model [28]. In order to determine the optimum number of hidden nodes, a series of topologies was used, in which the number of nodes varied from 1 to 9. The mean square error (MSE) was used as the error function. MSE measures the performance of the network, according to the following Equation:

$$MSE = \frac{\sum_{i=1}^{i=N} (y_{i,pred} - y_{i,\exp})^2}{N} \tag{8}$$

Where N is the number of data points, $y_{i,pred}$ is the network prediction, $y_{i,exp}$ is the experimental response and i is an index of data.

The primary goal of training is to minimize the error function (MSE) by searching for a set of connection weights and biases that causes the ANN to produce outputs that are equal or close to the target values. In other words, the backpropagation algorithm minimizes the MSE between the observed and the predicted output in the output layer, through two phases. In the forward phase, the external input information signals at the input neurons, which are propagated forward to compute the output information signal at the output neuron. In the backward phase, modifications to the connection strengths are made based on the basis of the difference in the predicted and observed information signals at the output neuron [17, 29].

Fig. 9 shows the MSE values versus the number of neurons in the hidden layer.

The commonly employed error function, root-mean-square error (RMSE) was used in this study, which can be defined as Equation (9):

$$RMSE = \sqrt{\frac{\sum_{i=1}^{N} \sum_{n=1}^{M} (y_n{}^i - \hat{y}_n{}^i)^2}{NM}}, \tag{9}$$

Where, N refers to the number of patterns used in the training; M denotes the number output nodes; i denotes the index of the input pattern and y^i_n and $\hat{y}^i_n$ are the actual and predicted outputs, respectively.

The MSE and RMSE values for overall model (test, validation and train) are shown in Fig.10.

The training, validation and testing of the model

The input data were divided into three groups such as training (60%), validation (20%) and testing (20%) for development of the model. Fig. 11 represents the model of ANN with better R^2 values of training (0.99966), validation (0.9953) and testing (0.98296). Fig. 11 represents that the overall model fit to linear equation with R^2 value 0.99664. Thus, the developed ANN model was able to accurately simulate dye degradation (target) and reproduce experimental results with greater precision. Dye degradation (target) has been precisely achieved

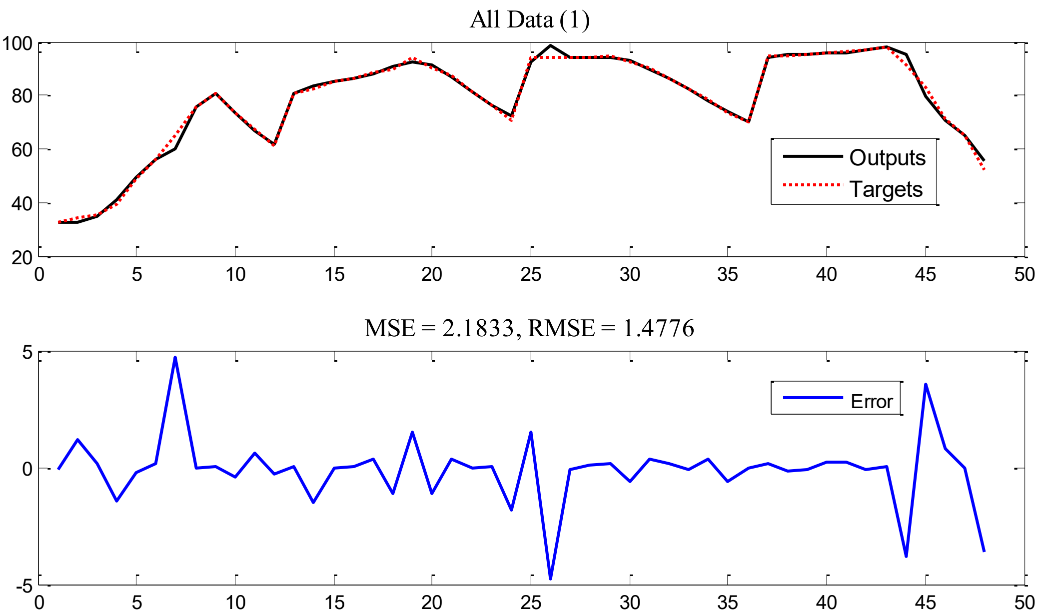

Fig. 10. The MSE and RMSE values for overall model in ANN.

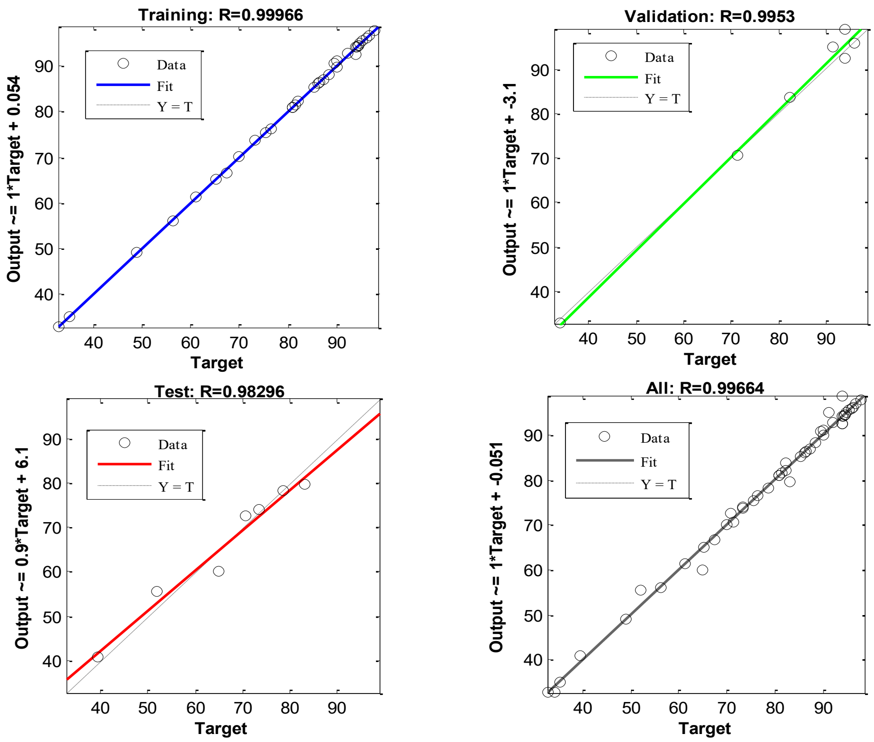

Fig. 11. Comparison between ANN derived and experimentally measured values of dye degradation for training, validation, testing and overall datasets.

by the incorporation of multilayered feed forward ANN, trained by back propagation algorithm, with significant R^2 values.

The ANN used in this paper, provided the weights listed in Table 3. The weights are coefficients between the artificial neurons, which are analogous to synapse strengths between the axons and dendrites in real biological neurons.

Table 3. Matrix of weights, W1: weights between input and hidden layers; W2: weights between hidden and output layers.

	W1					W2	
Neuron	Parameters				Bias	Neuron	Weight
	pH	Catalyst amount	Dye concentration	H_2O_2 concentration			
1	-0.66998	0.978137	-0.75728	-0.79586	0.436917	1	1.513845
2	-0.41256	-0.76985	1.922214	0.179188	-0.81222	2	-2.04786
3	0.821986	-0.88984	1.450019	-0.88439	0.765412	3	-1.43828
4	0.453235	0.511618	-0.01272	0.300039	-0.8578	4	0.225354
5	-0.50726	0.863626	-0.81169	0.558547	-0.2438	5	0.971305
6	-0.52779	-0.21484	0.316172	0.741835	0.908908	6	-0.04797
7	-0.47162	0.344342	-1.19212	0.080792	-0.08963	7	1.091656
8	0.519572	0.322119	-1.26523	0.261648	-0.22086	8	1.005401
9	0.949331	-1.48207	0.775707	0.834643	-1.2016	9	-2.01433
						Bias	0.359574

Table 4. Relative importance of input parameters on the value of dye degradation.

Input parameters	Importance (%)
pH	20.08677
Catalyst amount	26.22886
Dye concentration	37.82567
H_2O_2 concentration	15.8587

Therefore, each weight decides what proportion of the incoming signal will be transmitted into the neuron's body. Garson proposed an equation based on the partitioning of connection weights [30, 31]:

$$I_j = \frac{\sum_{m=1}^{m=N_h}\left(\left(\left|W_{j_m}^{j_h}\right| \Big/ \sum_{k=1}^{N_i}\left|W_{k_m}^{i_h}\right|\right)\times\left|W_{m_n}^{h_o}\right|\right)}{\sum_{k=1}^{k=N_i}\left\{\sum_{m=1}^{m=N_h}\left(\left|W_{k_m}^{i_h}\right| \Big/ \sum_{k=1}^{N_i}\left|W_{k_m}^{i_h}\right|\right)\times W_{m_n}^{h_o}\right\}} \tag{10}$$

where I_j is the relative importance of the j^{th} input variable on the output variable, N_i and N_h are the numbers of input and hidden neurons, respectively, W are connection weights, the superscripts i, h and o refer to input, hidden and output layers, respectively, and subscripts k, m and n refer to input, hidden and output neurons, respectively.

The importance of effective parameters on the photo degradation as calculated by Eq. (10) is shown in Table 4. As shown the importance values of the parameters was dye concentration > catalyst amount > pH > H_2O_2 concentration on the degradation process.

CONCLUSION

Fe_2O_3/BEN particles were successfully synthesized by precipitation method. Particles were characterized by SEM, XRD and BET techniques. The results demonstrated that the produced Fe_2O_3/BEN have sufficient properties as a photocatalyst for degradation of SYF dye. In this paper, dye photocatalytic degradation by model ANN with back propagation algorithm and four neurons in the input, seven neurons in the hidden and one neurons in the output was used. Various parameters affecting in the dye degradation process such as: pH, catalyst dosage, dye concentration and H_2O_2 concentration were analyzed and optimized. The results showed that pH= 4, catalyst amount=60 mg/L, dye concentration =50 ppm and H_2O_2 concentration =32 ppm was optimum conditions for this reaction. The most effective parameter in the photocatalytic degradation efficiency was dye concentration (37.8%). Comparison between data obtained from ANN method and experimental data indicated that the proposed ANN model provides reasonable predictive performance.

ACKNOWLEDGMENT

The author would like to gratefully acknowledge members of the Research Laboratory of Islamic Azad University, Tuyserkan Branch, Tuyserkan, Iran.

CONFLICT OF INTEREST

The authors declare that there is no conflict of interests regarding the publication of this manuscript.

REFERENCES

1. H. Zollinger, *Color: A Multidisciplinary Approach*, Verlag Helvetica Chimica Acta, Zurich (Switzerland) Wiley-VCH, 1999, p. 41.
2. M.E. Hassan, Y. Chen, G. Liu, D. Zhu and J. Cai, J. Water Proc. Eng. 12, 52-57 (2016).
3. T.A. Gad-Allah, Sh. Kato, Sh. Satokawa and T. Kojima, Desalination. 244, 1-11 (2009).
4. C.C. Wang, C.K. Lee, M.D. Lyu and L.C. Juang, Dyes Pigments. 76, 817-824 (2008).
5. R. Moradi and A. Ganjali, Russian J. Phys. Chem. A. 93, 2789-2797 (2019).
6. M. Nikazar, K. Gholivand and K. Mahanpoor, Desalination. 219, 293-300 (2008).
7. J. Saien and A.R. Soleymani, J. Hazard. Mater. 144, 506-512 (2007).
8. C. Galindo, P. Jacques and A. Kalt, J. Photochem. Photobiol. A: Chem. 130, 35-47 (2003).
9. M.A. Zayed, S.E. El-Begawy and H.E. Hassan, Arabian J. Chem. 10, 573-581 (2017).
10. D. Graupe, *Principles of Artificial Neural Networks*, Vol. 7, 2nd Edition, World Scientific, 2013, p. 1
11. S. Gob, E. Oliveros, S.H. Bossmann, A.M. Braun, R. Guardani and C.A.O. Nascimento, Chem. Eng. Proces. 38, 373-382 (1999).
12. V.K. Pareek, M.P. Brungs, A.A. Adesina and R. Sharma, J. Photochem. Photobiol. A: Chem. 149, 139-146 (2002).
13. S. Lek S and J.F. Guegan, Ecological Modelling. 120, 65-73 (1999).
14. C.H. Wen and C.A. Vassiliadis, Eng. Appl. Artificial Intelligence. 11, 685-705 (1998).
15. A. Ghaffari, H. Abdollahi, M. Khoshayand, I.S. Bozchalooi, A. Dadgar and M. Rafiee-Tehrani, Int. J. Pharm. 327, 126-138 (2006).
16. F. Despange and D.L. Massart, Analyst. 123, 157-178 (1998).
17. A. Aleboyeh, M.B. Kasiri, M.E. Olya and H. Aleboyeh, Dyes Pigments. 77, 288-294 (2008).
18. F. Chen, Y. Xie, J. Zhao and G. Lu, Chemosphere. 44, 1159-1168 (2001).
19. R. Moradi, Russian J. Phys. Chem. A. 92, 2781-2789 (2018).
20. J. Saien, M. Asgari, A.R. Soleymani and N. Taghavinia, Chem. Eng. J. 151, 295-301 (2009).
21. R. Moradi, M. Hamidvand and A. Ganjali, Russian J. Phys. Chem. A. 93, 1133-1142 (2019).
22. C. Zhu, L. Wang, L. Kong, X. Yang, L. Wang, S. Zheng, F. Chen, F. Maizhi and H. Zong, Chemosphere. 41, 303-309 (2000).
23. R. Moradi, A. Bodaghi, J. Hosseini and A. Gangali, Arch. Hyg. Sci. 8, 1–8 (2019).
24. M. Torkaman, R. Moradi and B. Keyvani, Revue Roumaine De Chimie. 61,763-772 (2016).
25. N. Daneshvar, D. Salari and A.R. Khataee, J. Photochem. Photobio. A. 157, 111-116 (2003).
26. R. Moradi and J. Hosseini, Arch. Hyg. Sci. 6, 326-332 (2017).
27. R. Moradi, A. Gangali, A.R. Yari and M.H. Mahmoudian, Arch. Hyg. Sci. 7, 288–294 (2018).
28. A. Duran and J.M. Monteagudo, Water Res. 41, 690-698 (2007).
29. M.M. Hamed, M.G. Khalafallah and E.A. Hassanien, Environ. Model. Software. 19, 919-928 (2004).
30. G.D. Garson, AI Expert. 6, 47-51 (1991).
31. A.R. Khataee and M.B. Kasiri, J. Mol. Catal. A Chem. 331, 86-100 (2010).